Linear instability in two-layer channel flow due to double-diffusive phenomenon

Kirti Chandra Sahu*
Department of Chemical Engineering, Indian Institute of Technology Hyderabad, India.
(Dated: January 8, 2020)

The linear stability characteristics of a pressure-driven channel flow of two miscible fluids flowing in a layered manner is investigated in the presence of two scalar components diffusing at different rates (double-diffusive (DD) phenomenon). The fluids are assumed to have the same density, but different viscosities. The parameters varied are the Reynolds number, Schmidt number, and thickness of the bottom layer. It is observed that the linear stability behaviour in the presence of DD effect is strikingly different from that observed in the single-component (SC) system. While the SC two-layer configuration is stable, the DD two-layer flow becomes unstable at low and moderate Reynolds numbers. It is found that increasing the diffusivity ratio of the faster to the slower diffusing scalar destabilises the system. A region of instability distinct from that of the Tollmien-Schlichting (TS) mode appears for some combinations of the log-mobility ratios of the slower and faster diffusing scalars. This unstable region grows as the diffusivity ratio increases and the thickness of the bottom layer decreases. For a constant diffusivity ratio, decreasing the Schmidt number of the slower diffusing scalar also increases the region of instability. An energy budget analysis is conducted to understand the underlying mechanism of this instability. Two mechanisms, namely- (i) the rate of energy transfer from the basic flow to the disturbance and (ii) the disturbance energy due to mean viscosity gradient are found to be the significant contributors to the increase in the rate of change of the disturbance kinetic energy.

I. INTRODUCTION

The flow of two liquid layers exhibits interesting instability patterns due to the variation in fluid properties, such as viscosity and density. Many researchers have studied this subject because of its importance in many industrial applications, e.g. crude oil transport in pipelines, polymer deposition and extrusion, food processing industries, to name a few [1–3]. Also in several geophysical and industrial applications, instability is caused by viscosity and density differences due to the coexistence of two scalars (e.g. temperature, salinity, etc.) diffusing at different rates, commonly referred to as the double-diffusive (DD) phenomenon. An example of DD phenomenon cab be observed in the distillation process of crude-oil in a refinery, which involves the asphaltenes-based deposit and temperature gradient. In such a situation, the asphaltenes-based deposit and temperature can serve as the slower and faster diffusing scalars, respectively. The temperature and salinity gradients can also be observed in the ocean. It is known that heat diffuses about 100 times faster than salt in water (i.e., the diffusivity ratio, $\delta = 100$). This leads to DD convection-driven instabilities in the ocean [1]. Although the scalars present in a system simultaneously contribute to the viscosity and density variations, the present study isolates the effects of viscosity contrast alone. An extensive review of instability in viscosity-stratified flows due to the DD convection can be found in Govindarajan and Sahu [4] and Sahu [5]. While several researchers have investigated the interfacial instability of two fluid layers with different viscosity and density separated by a sharp interface [6–12], in the present study, two-layer miscible channel flow in the presence of DD effect is investigated, which has not been in the past.

The instability associated with single-component (SC) flow is outlined before reviewing literature on the instability caused by the DD phenomenon. In a SC system, the viscosity-stratification is achieved with only one scalar. Miscible flows are characterised primarily by diffusivity (i.e. the inverse of the Schmidt number). The influence of diffusivity on the instability in three-layer Poiseuille channel flow, which is analogous to core-annular configuration in pipe flow [2, 13, 14], has been studied by several researchers, e.g. [15–17]. Their main findings are as follows. When the viscosity decreases (increases) towards the wall, channel flow is substantially stabilised (destabilised) at low to moderate Schmidt numbers with respect to the constant-viscosity (CV) system. These effects are accentuated by increasing the viscosity contrast. On the other hand, at high Schmidt numbers, the existence of a mixed layer of fluid always leads to destabilisation, which increases with the Schmidt number. It was also found that both stabilisation and destabilisation observed in SC channel flow are far larger when the critical layer of the dominant eigenmode overlaps with the viscosity stratified layer [18]. At the critical layer, the phase velocity of the disturbance is equal to the mean streamwise velocity at which significant kinetic energy production occurs. The SC channel flow was also found to be absolutely unstable for a range of the viscosity ratios and Reynolds numbers [19].

* ksahu@iith.ac.in

Few researchers [20, 21] have also studied the linear stability behaviour of the two-layer SC miscible channel flow with the aim of comparing it with the corresponding interface configuration. In the Stokes flow regime, Talon and Meiburg [20] found that instability depends on the position of the mixed layer, and the reason for the instability observed was the disturbance of the concentration relative to the interface. Sahu and Govindarajan [21] studied the instability in the inertial regime and found a region of instability distinct from that of the Tollmien-Schlichting (TS) mode at low and moderate Reynolds numbers due to the overlap of the mixed layer with the critical layer of the dominant disturbance. They focused on the situation when the viscosity increases towards the less wide layer.

Next, the earlier studies on instability due to DD effect are reviewed. The instability in the presence of DD phenomenon has been extensively studied in porous media and displacement flows (see for instance, [22–25]). Considering a stable configuration in a three-layer SC channel flow (i.e. when the fluid layer near the wall is less viscous than the fluid layer at the center of the channel), Sahu and Govindarajan [26] found another mode of instability driven by the DD effect in addition to the TS mode. The DD mode becomes stronger as the diffusivity ratio of the two scalars increases. Extending this study, they [27] also demonstrated the existence of a fast-growing absolute instability, which is only convectively unstable without the involvement of DD phenomenon. Ghosh et al. [28] explored the effect of wall velocity slip on the DD instability mode observed in the previous study [26].

The effect of the thickness of the mixed layer, q in two-layer SC [20, 21] and three-layer DD [26] configurations has also been thoroughly investigated. It was reported that decreasing the mixed layer thickness is always destabilising and the flow behaviour resembles the interfacial flow with zero surface tension in the limiting case, $q \to 0$.

As the above brief review shows, the DD effect on the linear instability in pressure-driven two-layer channel flow with a mixed layer in between has not been conducted yet, which is the subject of present work. Refs. [20, 21] reported their findings on the linear stability characteristics of two-layer SC system with the viscosity increasing towards the less wide layer. They expected this situation to be more unstable compared to the situation when viscosity decreases towards the wall as observed in three-layer systems. However, it is shown here that this assumption is not true for all the parameters. As the effect of the mixed layer is well understood and its behaviour is found to be similar here as well, the parameters varied in the present work are the Reynolds number, Schmidt number, and height of the mixed layer from the bottom wall. For the range of parameters considered, it is observed that the linear stability behaviour in the presence of DD effect is strikingly different from that observed in the single-component (SC) two-layer channel flow. While the SC two-layer configuration is stable, the DD two-layer flow becomes unstable at low and moderate Reynolds numbers. Increasing the diffusivity ratio of the faster to the slower diffusing scalar is found to enhance the linear instability. Depending on the sign of the log-mobility ratios of the slower and faster diffusing scalars, a distinct unstable region is observed due to the DD effect, which is more pronounced at high Schmidt numbers and as the width of the bottom layer is decreased. An energy budget analysis is conducted to understand the underlying mechanism of the DD instability.

The rest of the paper is structured as follows: Section II describes the mathematical formulation of the basic state and the linear stability analysis. The energy budget analysis of the disturbance is also done in Section II. The results of linear stability are discussed in Section III, and the final remarks are given in Section IV.

II. FORMULATION

The linear stability characteristic in pressure-driven two-layer channel flow of two miscible fluids in the presence of double-diffusive (DD) phenomenon is considered. The schematic of the flow configuration is shown in Fig. 1. The fluids are assumed to be Newtonian and incompressible. The two-dimensional Cartesian coordinate system (x, y) is used to model the flow behaviour, where x and y denote the streamwise and wall-normal coordinates, respectively. The rigid and impermeable channel walls are located at $y = 0, H$. Each fluid consists of two different proportions of scalars, S and F, representing respectively the slower and faster diffusing scalars. For example, in Fig. 1, fluid 1 and fluid 2 can be fresh-cold water and salty-warm water, respectively. Here, temperature and salt represent the faster and slower diffusing scalars, respectively. Mathematically, Fluid '1' (having viscosity μ_1; scalars S and F in quantity S_1 and F_1) and fluid '2' (having viscosity μ_2; scalars S and F in quantity S_2 and F_2) occupy the regions $h + q \leq y \leq H$ and $0 \leq y \leq h$, respectively. The fluids are separated by a mixed layer of uniform thickness q, which is based the parallel flow approximation as used by the previous studies [13, 26, 29] (also see justification given in Appendix). To isolate the effects of viscosity, it is assumed that the density, ρ of the fluids is the same.

The dynamics viscosity, μ is assumed to be an exponential function of the concentration of the scalars as follows

$$\mu = \mu_1 \exp\left[R_s\left(\frac{S - S_1}{S_2 - S_1}\right) + R_f\left(\frac{F - F_1}{F_2 - F_1}\right)\right], \tag{1}$$

where $R_s\,(\equiv (S_2 - S_1)d(\ln\mu)/dS)$ and $R_f\,(\equiv (F_2 - F_1)d(\ln\mu)/dF)$ are the log-mobility ratios of the slower and faster diffusing scalars, respectively. R_s and R_f are essentially like logarithms of viscosity ratios due to the presence of

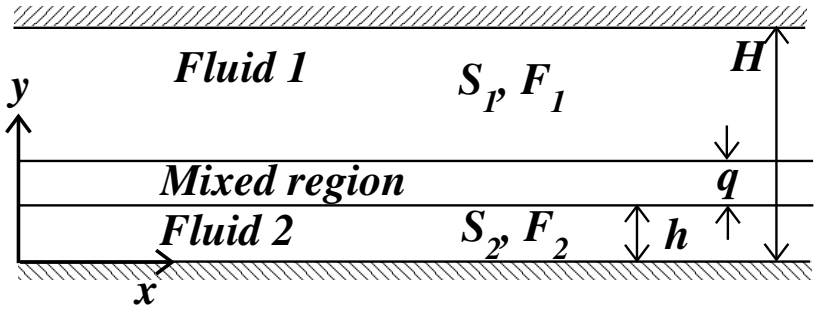

FIG. 1: Schematic of the two-layer flow configuration (not to scale). Fluids '2' and '1' occupy the regions $0 \leq y \leq h$ and $h+q \leq y \leq H$ of the channel, respectively, and they are separated by a mixed layer of uniform thickness q.

scalars s and f separately. Note that such a function for viscosity has been widely used to study viscosity-related instabilities (e.g. [3, 22, 30].

The flow dynamics is governed by the continuity, Navier-Stokes equations together with the convection-diffusion equations for both the scalars, which are given by

$$\nabla \cdot \mathbf{u} = 0, \tag{2}$$

$$\rho\left[\frac{\partial \mathbf{u}}{\partial t} + \mathbf{u}\cdot\nabla\mathbf{u}\right] = -\nabla p + \nabla\cdot\left[\mu(\nabla\mathbf{u} + \nabla\mathbf{u}^T)\right], \tag{3}$$

$$\frac{\partial S}{\partial t} + \mathbf{u}\cdot\nabla S = \mathcal{D}_s\nabla^2 S, \tag{4}$$

$$\frac{\partial F}{\partial t} + \mathbf{u}\cdot\nabla F = \mathcal{D}_f\nabla^2 F, \tag{5}$$

where $\mathbf{u} \equiv (u, v)$ is the two-dimensional velocity vector, wherein u and v are the velocity components in the streamwise (x) and wall-normal (y) directions, respectively; t denotes time; p represents pressure; $\mathcal{D}_s$ and $\mathcal{D}_f$ are the diffusion coefficients of the slower and faster diffusing scalars, respectively. Thus $\mathcal{D}_f > \mathcal{D}_s$ and $\delta(\equiv \mathcal{D}_f/\mathcal{D}_s) \geq 1$. In the current formulation, by setting $\delta = 1$ and the value of one log-mobility ratio to zero, one gets the single-component (SC) two-layer system as considered in Refs. [20, 21].

The following scaling is used to make the governing equations dimensionless:

$$(x, y, q, h) = H\left(\widetilde{x}, \widetilde{y}, \widetilde{q}, \widetilde{h}\right),\ t = \frac{H^2}{Q}\widetilde{t},\ (u, v) = \frac{Q}{H}(\widetilde{u}, \widetilde{v}),\ p = \frac{\rho Q^2}{H^2}\widetilde{p},$$
$$\mu = \widetilde{\mu}\mu_1,\ \widetilde{s} = \frac{S - S_1}{S_2 - S_1},\ \widetilde{f} = \frac{F - F_1}{F_2 - F_1}, \tag{6}$$

where tildes designate the dimensionless quantities and Q denotes the total volume flow rate per unit distance in the spanwise direction. After dropping the tilde notations, the dimensionless governing equations are given by

$$\nabla \cdot \mathbf{u} = 0, \tag{7}$$

$$\left[\frac{\partial \mathbf{u}}{\partial t} + \mathbf{u}\cdot\nabla\mathbf{u}\right] = -\nabla p + \frac{1}{Re}\nabla\cdot\left[\mu(\nabla\mathbf{u} + \nabla\mathbf{u}^T)\right], \tag{8}$$

$$\frac{\partial s}{\partial t} + \mathbf{u}\cdot\nabla s = \frac{1}{ReSc}\nabla^2 s, \tag{9}$$

$$\frac{\partial f}{\partial t} + \mathbf{u}\cdot\nabla f = \frac{\delta}{ReSc}\nabla^2 f, \tag{10}$$

where $Re(\equiv \rho Q/\mu_1)$ is the Reynolds number and $Sc(\equiv \mu_1/\rho\mathcal{D}_s)$ is the Schmidt number of the slower diffusing scalar. The effective Schmidt number of the faster diffusing scalar is Sc/δ. Note that in the present study, the Péclet number, $Pe(\equiv ReSc) >> 1$.

A. Basic state

The basic state (designated by upper case letters for the flow variables and subscript 0 for viscosity, s and f) is a steady, parallel and fully-developed flow, so $U = U(y)$, $V = 0$, $s_0 = s_0(y)$, $f_0 = f_0(y)$ and P is linear in x. Thus, the basic state streamwise velocity profile is given by

$$Re\left(\frac{dP}{dx}\right) = \frac{d}{dy}\left(\mu_0 \frac{dU}{dy}\right), \tag{11}$$

where $\mu_0 = e^{(R_s s_0 + R_f f_0)}$. Eq. (11) is solved using no-slip and no-flux conditions at the walls and dP/dx is obtained from the constant volumetric flow condition, $\int_0^1 U dz = 1$.

It is reasonable to assume that the scalars, s_0 and f_0, and their first and second derivatives are continuous at $y = h$ and $y = h + q$. Therefore, a smooth function such as a fifth order polynomial in the mixed layer can be chosen [15] to represent the variations of s_0 and f_0, which are given by

$$\begin{aligned} s_0 = f_0 &= 1, \qquad 0 \le y \le h, \\ s_0 = f_0 &= \sum_{i=1}^{6} a_i y^{i-1}, \quad h \le y \le h+q, \\ s_0 = f_0 &= 0, \qquad h+q \le y \le 1, \end{aligned} \tag{12}$$

where the constants a_i's $(i = 1, 6)$ are given by

$$\begin{aligned} a_1 = \frac{(h+q)^3}{q^5}\left[6h^2 - 3hq + q^2\right], \quad a_2 = -\frac{30h^2}{q^5}(h+q)^2, \quad a_3 = \frac{30}{q^5}h(h+q)(2h+q), \\ a_4 = -\frac{10}{q^5}\left[6h^2 + 6hq + q^2\right], \quad a_5 = \frac{15}{q^5}(2h+q) \quad \text{and} \quad a_6 = -\frac{6}{q^5}. \end{aligned} \tag{13}$$

In our previous study [21], it was shown that the results obtained using other fairly smooth profiles and Eqs. (12) and (13) are virtually indistinguishable.

B. Linear Stability analysis

In this section, the temporal linear stability equations are derived by splitting each flow variable into the basic-state quantity and a two-dimensional disturbance (designated by hat) using normal mode analysis as

$$(u, v, p, s, f, \mu)(x, y, t) = (U(y), 0, P, s_0(y), f_0(y), \mu_0(y)) + (\hat{u}, \hat{v}, \hat{p}, \hat{s}, \hat{f}, \hat{\mu})(y) e^{\mathrm{i}(\alpha x - \omega t)}. \tag{14}$$

Here $\mathrm{i} \equiv \sqrt{-1}$, α is the wavenumber and $\omega (\equiv \alpha c)$ denotes the frequency of the disturbance; c being the phase speed. In temporal stability analysis, α and ω are treated as real and complex quantities, respectively, such that for an unstable (stable) mode $\omega_i > 0$ ($\omega_i < 0$) and $\omega_i = 0$ represents a neutrally stable mode. The perturbation viscosity, $\hat{\mu}$ is given by

$$\hat{\mu} = \frac{\partial \mu_0}{\partial s_0}\hat{s} + \frac{\partial \mu_0}{\partial f_0}\hat{f}. \tag{15}$$

The linear stability equations are derived using the standard procedure [31], namely (i) substituting Eq. (14) into Eqs. (7)-(10), (ii) subtracting the basic state equations from the resultant equations, (iii) linearising and elimination of the pressure perturbation, (iv) re-expressing the amplitude of the velocity disturbances in terms of streamfunction $[(\hat{u}, \hat{v}) = (\psi', -\mathrm{i}\alpha\psi)]$. The final form of the linear stability equations (after suppressing the hat notation) are given by

$$\begin{aligned} \mathrm{i}\alpha Re\left[\left(\psi'' - \alpha^2\psi\right)(U-c) - U''\psi\right] &= \mu_0\left(\psi^{iv} - 2\alpha^2\psi'' + \alpha^4\psi\right) + \\ 2\mu_0'\left(\psi''' - \alpha^2\psi'\right) + \mu_0''\left(\psi'' + \alpha^2\psi\right) &+ U'\left(\mu'' + \alpha^2\mu\right) + 2U''\mu' + U'''\mu, \end{aligned} \tag{16}$$

$$\mathrm{i}\alpha ReSc\left[(U-c)s - \psi s_0'\right] = \left[s'' - (\alpha^2 + \beta^2)s\right], \tag{17}$$

$$\mathrm{i}\alpha ReSc\left[(U-c)f - \psi f_0'\right] = \delta\left[f'' - (\alpha^2 + \beta^2)f\right], \tag{18}$$

where the prime denotes differentiation with respect to y. The boundary conditions at walls of the channel ($y = 0, 1$) are given by

$$\psi \;=\; \psi' = s = f = 0. \tag{19}$$

Eqs. (16)-(18) together with the boundary conditions (Eq. (19)) constitute an eigenvalue problem of the form $AX = \omega BX$, where $X = [\psi, s, f]^T$ and ω are eigenvectors and eigenvalue, respectively. The Chebyshev spectral collocation [32] is employed to discretise and the public domain software, LAPACK is used to solve the linear stability equations. Since the gradients are high in the mixed region, the numerical accuracy requires more grid points, which can be accomplished with the following stretching function [33]:

$$y_j = \frac{a}{\sinh(by_0)}\left[\sinh\left\{(y_c - y_0)b\right\} + \sinh(by_0)\right], \tag{20}$$

where y_j are the locations of the grid points, a is the mid-point of the mixed layer, y_c is the Chebyshev collocation point, which is defined as $y_c = 0.5\cos\left\{\left[\frac{\pi(j-1)}{(n-1)}\right] + 1\right\}$, where n is the number of collocation points.

$$y_0 = \frac{0.5}{b}\ln\left[\frac{1 + (e^b - 1)a}{1 + (e^{-b} - 1)a}\right], \tag{21}$$

where the value of the degree of the clustering, b is taken as 8.

C. Numerical procedure and validation

The dependence of our numerical solutions on mesh refinement is examined to inspire confidence in the predictions of the linear stability analysis. The dispersion curves (ω_i versus α) obtained using different numbers of collocation points are presented in Fig. 2 for $Re = 1000$, $Sc = 10$, $h = 0.1$, $q = 0.1$, $R_s = -3.1$, $R_f = 3$ and $\delta = 2$. It can be seen that for different values of the order of Chebyshev polynomials (i.e., $n = 121$, 151 and 201), the dispersion curves are indistinguishable and therefore $n = 121$ is used to generate the remaining results presented in this study. Moreover, comprehensive validation exercises have been performed (not shown) by comparing the results obtained using the current code with the previous literature on three-layer [33] and core-annular configurations [13]. For further information, we refer the reader to our previous studies [21, 26].

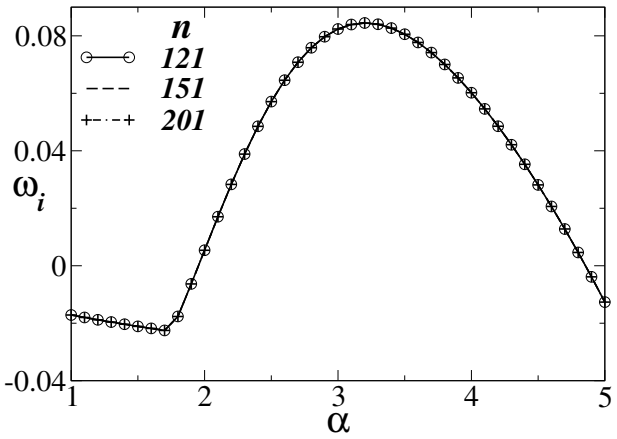

FIG. 2: Effect of number of the collocation points on the calculation of the growth rate of the disturbance (ω_i) for a typical set of parameters considered in the present study ($Re = 1000$, $Sc = 10$, $h = 0.1$, $q = 0.1$, $R_s = -3.1$, $R_f = 3$ and $\delta = 2$).

D. Energy budget analysis

An energy budget analysis is conducted to understand the mechanism of instability in two-layer channel flow due to the double-diffusive convection. A similar analysis was previously used by Sahu et al. [19] in the case of single-component three-layer miscible channel flow. The procedure followed to derive the energy budget equation are (i)

The inner product of the perturbed Navier-Stokes equations with the perturbation velocity vector is taken. (ii) The resulting equations are then added and integrated over the control volume. (iii) The volume integrals are then converted to surface integrals using divergence theorem. The final form of the energy budget equation is given by

$$KEN = REY + DIS + A + F + B, \tag{22}$$

where

$$KEN = \frac{1}{\lambda}\frac{d}{dt}\int_0^1 dy \int_0^\lambda dx \left[\frac{1}{2}(\hat{u}^2 + \hat{v}^2)\right],$$

$$REY = \frac{1}{\lambda}\int_0^1 dy \int_0^\lambda dx \left[-\hat{u}\hat{v}\frac{dU}{dy}\right],$$

$$DIS = -\frac{1}{\lambda Re}\int_0^1 dy \int_0^\lambda \mu_0 dx \left[2\left(\frac{\partial \hat{u}}{\partial x}\right)^2 + \left(\frac{\partial \hat{u}}{\partial y} + \frac{\partial \hat{v}}{\partial x}\right)^2 + 2\left(\frac{\partial \hat{v}}{\partial y}\right)^2\right],$$

$$A = \frac{1}{\lambda}\int_0^1 dy \int_0^\lambda dx \left[\frac{d\mu_0}{dy}\frac{\partial \hat{v}^2}{\partial y}\right],$$

$$F = -\frac{1}{\lambda Re}\int_0^1 dy \int_0^\lambda dx \left[\hat{u}\hat{\mu}\frac{d^2U}{dy^2}\right],$$

$$B = B_x + B_y = \frac{1}{\lambda Re}\int_0^1 dy \int_0^\lambda dx \left[\hat{v}\frac{\partial \hat{\mu}}{\partial x}\frac{dU}{dy}\right] + \frac{1}{\lambda Re}\int_0^1 dy \int_0^\lambda dx \left[\hat{u}\frac{\partial \hat{\mu}}{\partial y}\frac{dU}{dy}\right],$$

Here, KEN is the temporal rate of change in kinetic energy disturbance, so that $KEN > 0$ implies instability; REY denotes the "Reynolds-stress" term, which determines the rate of transfer of energy from the basic flow to the disturbance; DIS corresponds to the viscous dissipation of energy. The term A represents the disturbance energy due to mean viscosity gradient; B and F are the disturbance energies due to the gradient of viscosity perturbation and viscosity perturbation, respectively. The term B can be further decomposed into B_x and B_y, where B_x and B_y are the disturbance energies associated with the gradient of viscosity perturbation in x and y directions, respectively.

III. RESULTS AND DISCUSSION

As discussed in the Section I, single-component (SC) core-annular miscible channel flows are well known to become linearly unstable at low Reynolds numbers when the viscosity gradually increases towards both walls. On the other hand, huge stabilisation occurs in the opposite situation, i.e. when the viscosity decreases towards the walls (see for instance [2, 17–19, 34]). Two-layer SC miscible channel flow was also studied by Sahu and Govindarajan [21]; Talon and Meiburg [20]. Concentrating on the situation when the viscosity increases towards one wall (as shown in Fig. 3a for $R_s = 0.1$), Sahu and Govindarajan [21] found a region of instability distinct from that of the Tollmien–Schlichting (TS) mode at moderate Reynolds numbers due to the overlap of the mixed layer with the critical layer of the dominant disturbance. Mathematically, the SC configuration considered in Refs. [20, 21] can be obtained in the present double-diffusive (DD) formulation by setting $\delta = 1$ and $R_f = 0$. Unlike in core-annular flows, the stability behaviour due to the direction of viscosity-stratification (sign of R_s) is not obvious in two-layer systems. Therefore, the dispersion curves (ω_i versus α) are plotted in Fig. 3b for $R_s = -0.1$, 0 and 1 in the case of SC two-layer miscible channel flow before addressing the instability caused by the double-diffusive phenomenon which is the main subject of the present study. The rest of the parameters in Fig. 3b are $Re = 10^4$, $Sc = 10$, $h = 0.1$ and $q = 0.1$. Surprisingly, in this case, the behaviour of linear stability is the opposite of what is expected. It can be seen in Fig. 3b that the growth-rate, ω_i of the disturbance for $R_s = -0.1$ (i.e. when viscosity decreases towards the bottom wall) is higher than that for $R_s = 0.1$ (i.e. when viscosity increases towards the bottom wall). This is true, of course, when the bottom layer's width is less than the top layer.

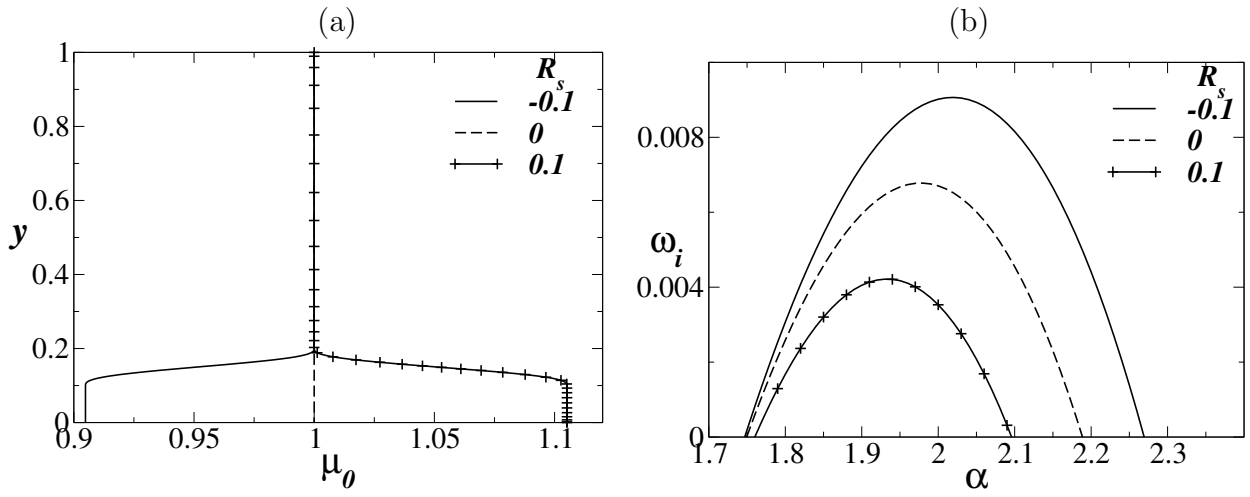

FIG. 3: (a) The basic state profiles of μ_0 and (b) the dispersion curves (ω_i versus α) for different values of R_s in a SC system ($R_f = 0$). The rest of the parameter values are $Re = 10^4$, $Sc = 10$, $h = 0.1$ and $q = 0.1$.

Next, the instability in the presence of double-diffusive phenomenon is examined for situations when the viscosity decreases towards the bottom wall ($R_s + R_f < 0$) in the two-layer miscible channel flow (Fig. 1) with the top layer (fluid '1') wider than the bottom layer (fluid '2'). In Figs. 4a and 4b, the neutral stability curves (along which $\omega_i = 0$) are plotted for different values of δ for ($R_s = 3$ and $R_f = -3.1$) and ($R_s = -3.1$ and $R_f = 3$), respectively. The plots also demarcate the stable and unstable regions. The rest of the parameter values used to generate Figs. 4a and 4b are $Sc = 10$, $h = 0.1$ and $q = 0.1$. Following the previous discussion on the stability characteristic in two-layer SC system, we can say that R_s is stabilising (destabilising) and R_f destabilising (stabilising) relative to the case of the constant-viscosity (CV) in Fig. 4a (Fig. 4b). However, the net stratification is destabilising in both the cases as $R_s + R_f < 0$. The neutral stability curve for the CV case (shown by red-dotted line in each panel) predicts the critical Reynolds number (the minimum value of Re at which the flow becomes linearly unstable) for the TS mode, $Re_{cr,TS}$ to be 7696.2, which is consistent with the value given in Drazin and Reid [35]. Note that, in the present study, the Reynolds number is defined based on the average velocity and channel height.

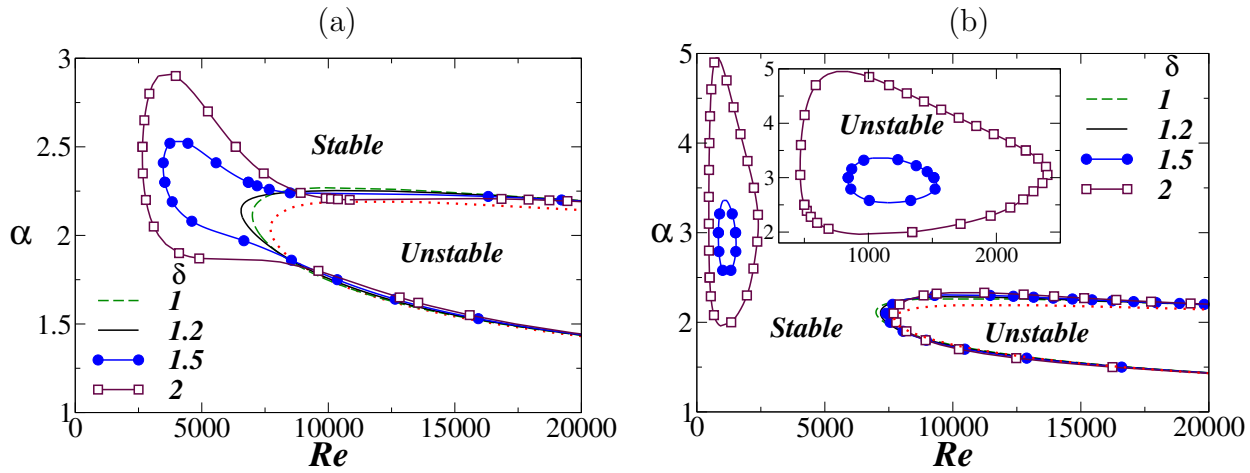

FIG. 4: The neutral stability curves for different values of δ. (a) $R_s = 3$ and $R_f = -3.1$ and (b) $R_s = -3.1$ and $R_f = 3$. The neutral stability curve for the TS mode (the constant-viscosity case) is shown by the red-dotted line ($Re_{cr,TS} = 7696.2$). The rest of the parameters values are $Sc = 10$, $h = 0.1$ and $q = 0.1$.

It can be seen in Fig. 4a that for $\delta = 1$ (SC system) the neutral stability curve is marginally moved to the left side of the TS mode, thus reducing the value of Re_{cr} relative to the TS mode. This is purely due to the presence of the unstable viscosity stratification ($R_s + R_f = -0.1$). In the case of DD system ($\delta > 1$), increasing the value of δ increases the unstable region and decreases the value of the critical Reynolds number. It can be seen that a 'neck' is formed in the neutral stability curve for $\delta = 2$ due to the DD effect. This effect is more pronounced for $R_s = -3.1$

and $R_f = 3$ as shown in Fig. 4b. In this case, in addition to the TS mode, another distinct mode due to the DD convection is clearly visible for $\delta \geq 1.5$ (see the closed unstable regions in Fig. 4b).

Close inspection of Figs. 4a and 4b also reveals that the values of Re_{cr} for $R_s = -3.1$ and $R_f = 3$ (Fig. 4b) are much lower than the $R_s = 3$ and $R_f = -3.1$ (Fig. 4a) for $\delta \geq 1.5$. This behaviour can be explained as follows. In Fig. 4a, the slower diffusing scalar, s is stabilising ($R_s > 0$) but the faster diffusing scalar, f is destabilising ($R_f < 0$). Thus, one can imagine that as the time progresses, the scalar f will diffuse out faster leaving only the scalar s in the system, which has a stabilising influence. On the other hand, opposite happens in Fig. 4b as the scalar s has a destabilising influence. However, as $Pe >> 1$ in the present study, the time scale of mixing is much smaller than the flow time scale and always there is a competition between these scalars to influence the stability behaviour.

In Figs. 5a and 5b, the dispersion curves for different values of δ are plotted for ($R_s = -3.1$ and $R_f = 3$) and ($R_s = -3.1$ and $R_f = 3$), respectively. The Reynolds numbers taken in Figs. 5a and 5b are 5000 and 1000, respectively. The rest of the parameter values are the same as those used in Fig. 4. It can be seen in Figs. 5a and 5b that for $\delta \geq 1.5$ the dispersion curves exhibit paraboloidal shapes, and $\omega_i > 0$ over a finite band of wavenumbers, indicating the presence of a linear instability. The maximum growth rate of the disturbance, $\omega_{i,max}$ and the region of instability (the range of unstable α) increase as the value of δ increases. Comparison of the dispersion curves depicted in Figs. 5a and 5b also reveals that the value of $\omega_{i,max}$ for a fixed δ value for ($R_s = -3.1$ and $R_f = 3$) is higher than that for ($R_s = -3.1$ and $R_f = 3$). This is in accordance with finding presented in Figs. 4a and 4b.

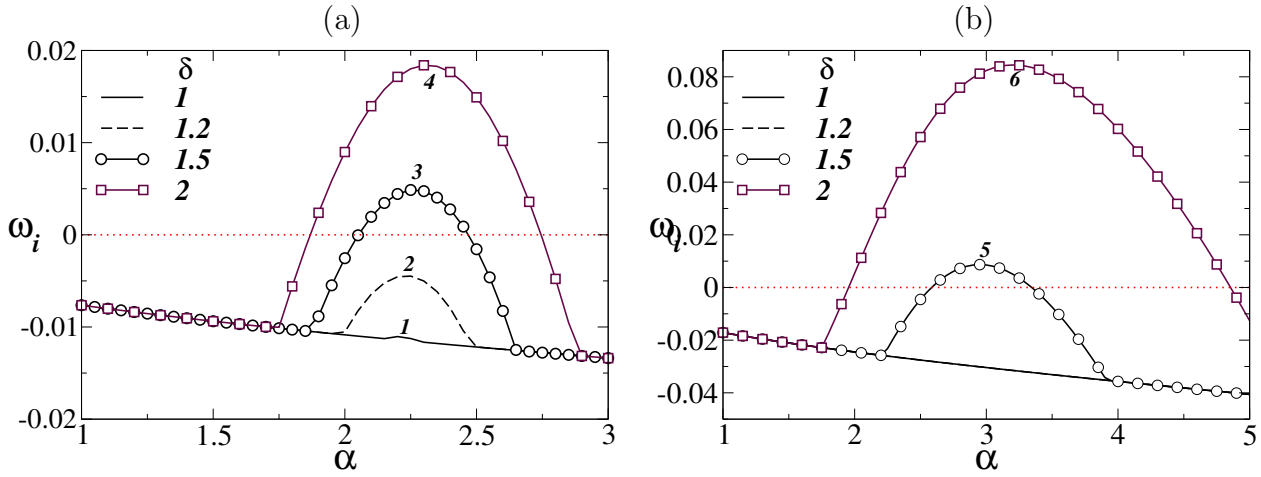

FIG. 5: The dispersion curves (ω_i versus α) for different values of δ. (a) $R_s = 3$ and $R_f = -3.1$ at $Re = 5000$ and (b) $R_s = -3.1$ and $R_f = 3$ at $Re = 1000$. The rest of the parameter values are $Sc = 10$, $h = 0.1$ and $q = 0.1$. The red-dotted line in each panel represents $\omega_i = 0$.

In order to gain insight on the mechanism of the instability observed due to DD phenomenon, in Tables I and II, the breakdown of KEN into its constituent components associated with the maximal temporal growth rate ($\omega_{i,max}$) for different values of δ (marked as points '1', '2', '3' and '4' in Fig. 5a, and points '5' and '6' in Fig. 5b) for ($R_s = 3$, $R_f = -3.1$, $Re = 5000$) and ($R_s = -3.1$, $R_f = 3$, $Re = 1000$) are presented, respectively. The rest of the parameters are the same as those used in Fig. 5. Inspection of Tables I and II reveals that $KEN > 0$ when $\omega_{i,max}$ is positive (i.e., for unstable modes) and increasing δ increases the value of KEN. It can be seen that the largest contributor to instability is due to REY, which is the the rate of transfer of energy from the basic flow to the disturbance (the "Reynolds-stress" term). The next largest contributor to instability is due to A, which is the disturbance energy due to mean viscosity gradient. It can be observed that the values of REY and A are increased as the value of δ increases, thereby destabilising the flow. The terms B_y (disturbance energies associated with the gradient of viscosity perturbation in the wall normal direction) and F (disturbance energy due to viscosity perturbation) also make positive, although small, contribution to KEN. The viscous dissipation (DIS) and the disturbance energy associated with the gradient of viscosity perturbation in the x direction provide negative contributions to the instability (i.e., stabilises the flow). Another observation is, for each value of δ, the value of KEN for ($R_s = -3.1$, $R_f = 3$) is higher than that of ($R_s = 3$, $R_f = -3.1$), even though the value of Re is smaller in the former as compared to the later, indicating that ($R_s = -3.1$, $R_f = 3$) is more unstable than ($R_s = 3$, $R_f = -3.1$). This can also be observed in Fig. 5.

Next, the effect of the location of the mixed layer, h on the neutral stability boundary due to the DD phenomenon is investigated in Figs. 6a and 6b for ($R_s = 3$ and $R_f = -3.1$) and ($R_s = -3.1$ and $R_f = 3$), respectively. The rest of the parameter values are $Sc = 10$, $q = 0.1$ and $\delta = 2$. In Fig. 6a, the slow diffusing scalar is stabilising and the fast diffusing scalar is destabilising, whereas in Fig. 6b, the slow diffusing scalar is destabilising and the fast diffusing

Points	*KEN*	*REY*	*DIS*	*A*	B_x	B_y	*F*
1	-0.049	0.170	-0.384	0.162	-0.0004	0.001	0.002
2	-0.020	0.239	-0.433	0.171	-0.0004	0.001	0.002
3	0.022	0.321	-0.473	0.171	-0.0005	0.001	0.003
4	0.087	0.467	-0.576	0.190	-0.0008	0.002	0.004

TABLE I: Energy budgets for the points labeled as 1, 2, 3 and 4 in Fig. 5(a).

Points	*KEN*	*REY*	*DIS*	*A*	B_x	B_y	*F*
5	0.0527	1.164	-1.732	0.429	-0.027	0.135	0.0829
6	0.5862	2.422	-2.997	0.689	-0.0627	0.387	0.1482

TABLE II: Energy budgets for the points labeled as 5, 6, 7 and 8 in Fig. 5(b).

scalar is stabilising if they are present alone in the system. However, in the presence of DD convection, the overall viscosity-stratification is destabilising in both the cases ($R_s + R_f < 0$). In Fig. 6a, it can be seen that for $h \geq 0.2$, the neutral stability curves look similar to that of the classical TS mode (the constant-viscosity case) as shown by red-dotted line. For $h = 0.2$, the critical Reynolds number decreases and the neutral stability curve exhibits a 'neck' near $Re_{cr,TS}$. Further decrease in the value of h results in a distinct region of instability, albeit small, at low Reynolds numbers. This effect is more prominent in Fig. 6b, where the distinct unstable regions can be seen for $h \leq 0.1$. Sahu and Govindarajan [26] have shown that this is due to the overlap of the mixed layer with the critical layer.

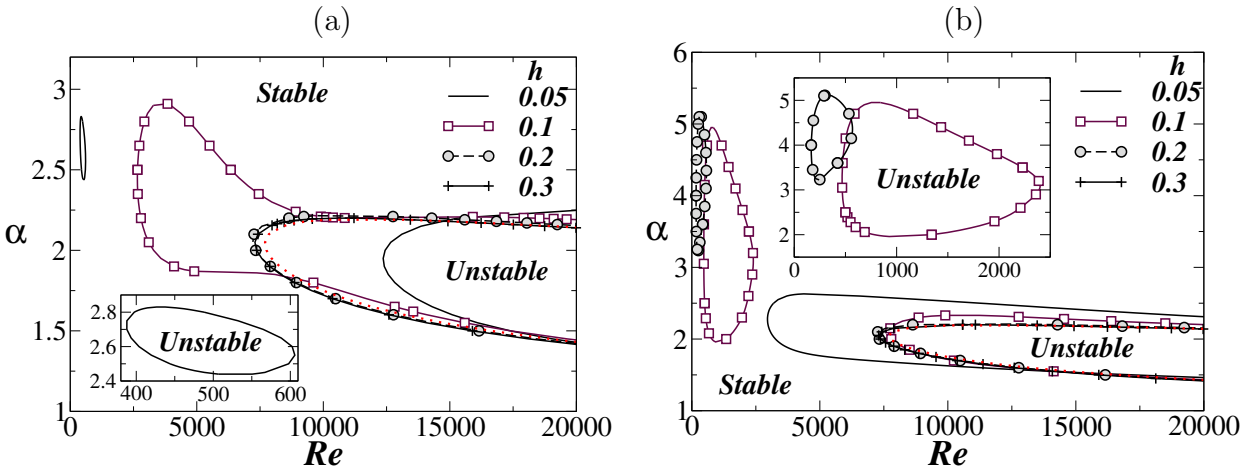

FIG. 6: The neutral stability curves for different values of h. (a) $R_s = 3$ and $R_f = -3.1$ and (b) $R_s = -3.1$ and $R_f = 3$. The neutral stability curve for the TS mode (the constant-viscosity case) is shown by the red-dotted line ($Re_{cr,TS} = 7696.2$). The rest of the parameter values are $Sc = 10$, $q = 0.1$ and $\delta = 2$.

Finally, the effect of the Schmidt number of the slower diffusing scalar with $\delta = 2$ is investigated in Figs. 7a and 7b for ($R_s = 3$ and $R_f = -3.1$) and ($R_s = -3.1$ and $R_f = 3$), respectively. It can be seen in Fig. 7a that increasing Sc (i.e. decreasing diffusivity of the slower diffusing scalar) increases the critical Reynolds number, but slowly. Also it can be observed that as we increase the value of Sc the tendency of necking increases. At $Sc = 30$, the distinct mode of instability due to the DD effect appears. As interfacial flow ($q \to 0$ and $Sc \to \infty$) is linearly unstable at any small Reynolds number, we can expect a non-monotonic effect of Sc as we increase the value of Sc further. However, this is not a subject of discussion here as this behaviour is already well known (see for instance Ref. [21]). In Fig. 7b, it can be seen that the distinct mode of instability (closed curve) at low Re appears for each value of Sc considered. Also due to the destabilising influence of the slower diffusing scalar, increasing Sc decreases the value of Re_{cr} slightly. Close inspection also reveals that increasing Sc shrinks the region of instability regime at low Re. This also indicates that the instability observed here is due to the DD effect in the miscible system.

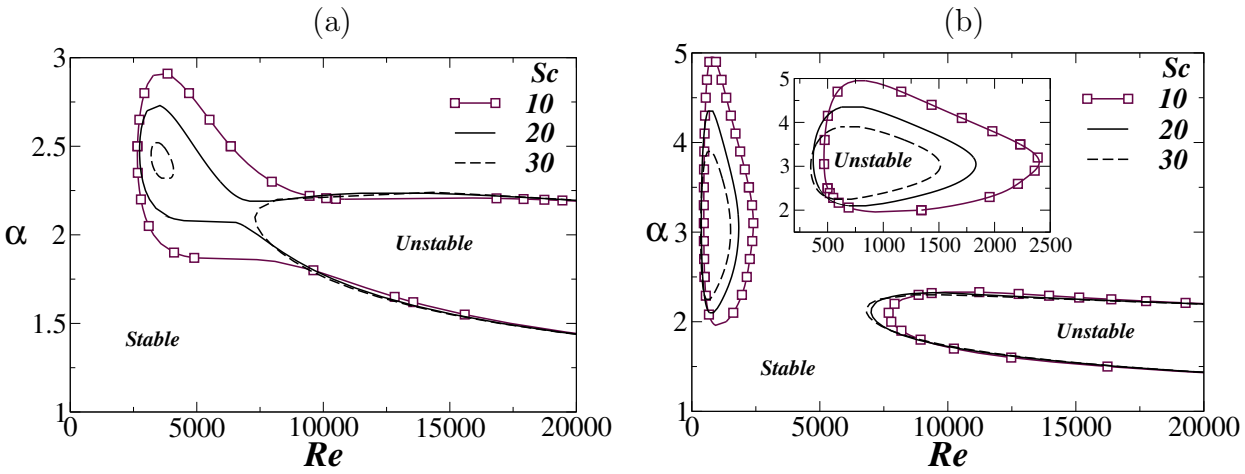

FIG. 7: The neutral stability curves for different values of Sc. (a) $R_s = 3$ and $R_f = -3.1$ and (b) $R_s = -3.1$ and $R_f = 3$. The rest of the parameter values are $h = 0.1$, $q = 0.1$ and $\delta = 2$.

IV. CONCLUDING REMARKS

In this study, the linear stability analysis of a pressure-driven channel flow of two miscible fluids in the presence of two scalars diffusing at different rates and affecting the fluid viscosity is performed. The fluids are assumed to have the same density in order to isolate the effect of viscosity stratification. The Reynolds number, Schmidt number and height of the mixed layer from the bottom wall are varied and their effects on the linear stability characteristics are investigated. It is observed that in the presence of DD effect, the linear stability behaviour is markedly different from the single-component two-layer channel flow. While the two-layer SC configuration is stable, it is shown that the two-layer DD flow is unstable at low and moderate Reynolds numbers. It is found that increasing the diffusivity ratio of the faster to the slower diffusing scalar destabilises the system. For some combinations of the log-mobility ratios of the slower and faster diffusing scalars, a region of instability distinct from that of the classical Tollmien-Schlichting mode appears at low and moderate Reynolds numbers. This unstable region grows as the diffusivity ratio increases and the thickness of the bottom layer decreases. For a constant diffusivity ratio, decreasing the value of the Schmidt number of the slower diffusing scalar also increases the region of instability. An energy budget analysis is carried out to understand the underlying mechanism of this instability and it is found that the rate of energy transfer from the basic flow to the disturbance and the disturbance energy due to the mean gradient of viscosity lead to the increase in the rate of change of the kinetic energy disturbance, i.e. to the observed instability.

Appendix: Validity of the parallel flow assumption

The validity of the parallel flow assumption used in the present study can be explained by analysing the flow with a splitter plate located at $x < x_0$ and fixed y that separates the parallel streams of two miscible fluids flowing on both sides of this plate. The streams come into contact with each other at $x = x_0$ and mix for $x > x_0$, thus producing a stratified layer. This layer's thickness (q) increases as the fluids move downstream, so q is a function of x. The scalars s_0 and f_0 governs by

$$\frac{\partial s_0}{\partial t} + U\frac{\partial s_0}{\partial x} + V\frac{\partial s_0}{\partial y} = \frac{1}{Pe}\left[\frac{\partial^2 s_0}{\partial x^2} + \frac{\partial^2 s_0}{\partial y^2}\right], \tag{23}$$

$$\frac{\partial f_0}{\partial t} + U\frac{\partial f_0}{\partial x} + V\frac{\partial f_0}{\partial y} = \frac{1}{Pe}\left[\frac{\partial^2 f_0}{\partial x^2} + \frac{\partial^2 f_0}{\partial y^2}\right]. \tag{24}$$

For slow diffusion (i.e for high Pe), we can assume that $V \ll U$ and $\frac{\partial^2}{\partial x^2} \ll \frac{\partial^2}{\partial y^2}$. Physically, this means that the variations of the gradients of the flow variables and the thickness q of the mixed region have much larger length scale than the disturbance wavelength. In such a scenario, s_0 and f_0 are function of y and t only and not of x. Thus the

above equations reduce to

$$\frac{\partial s_0}{\partial t} = \frac{1}{Pe}\frac{\partial^2 s_0}{\partial y^2}. \tag{25}$$

$$\frac{\partial f_0}{\partial t} = \frac{1}{Pe}\frac{\partial^2 f_0}{\partial y^2}. \tag{26}$$

We can also say that $U \sim O(1)$, $y \sim \sqrt{\nu}$, where ν is the kinematic viscosity. As the viscosity is directly proportional to the concentration of s_0 and f_0 in the mixed layer, $qs_0 \sim qf_0 \sim O(y^2)$. This implies that $\partial s_0/\partial x$ and $\partial f_0/\partial x$ are $\simeq \frac{1}{q}O(1/Pe)$. The change in the thickness of the mixed layer (q) along the x-direction is therefore very low for $Pe >> 1$. As in the present study, $Pe \geq 1000$, it is reasonable to assume uniform viscosity stratified layer thickness.

Acknowledgment

The author thanks Science and Engineering Research Board (SERB), India for providing financial support through the grant number, MTR/2017/000029.

[1] J. S. Turner, "Double-diffusive phenomena," Ann. Rev. Fluid Mech. **6**, 37 (1974).
[2] D. D. Joseph, R. Bai, K. P. Chen, and Y. Y. Renardy, "Core-annular flows," Ann. Rev. Fluid Mech. **29**, 65 (1997).
[3] C.-Y. Chen and E. Meiburg, "Miscible displacement in capillary tubes. Part 2. Numerical simulations," J. Fluid Mech. **326**, 57 (1996).
[4] R. Govindarajan and K. C. Sahu, "Instabilities in viscosity-stratified flows," Ann. Rev. Fluid Mech. **46**, 331 (2014).
[5] K. C. Sahu, "A review on double-diffusive instability in viscosity stratified flows," Proc. Indian Natn, Sci. Acad. **80**, 513 (2014).
[6] C. S. Yih, "Instability due to viscous stratification," J. Fluid Mech. **27**, 337 (1967).
[7] E. J. Hinch, "A note on the mechanism of the instability at the interface between two shearing fluids," J. Fluid Mech. **144**, 463 (1984).
[8] A. P. Hooper, "Long-wave instability at the interface between two viscous fluids: Thin layer effects," Phys. Fluids **28(6)**, 1613 (1985).
[9] A. P. Hooper and W. G. C. Boyd, "Shear flow instability at the interface between two fluids," J. Fluid Mech. **128**, 507 (1983).
[10] K. C. Sahu and O. K. Matar, "Three-dimensional linear instability in pressure-driven two-layer channel flow of a Newtonian and a Herschel-Bulkley fluid," Phys. Fluids **22**, 112103 (2010).
[11] P. Valluri, L. O. Naraigh, H. Ding, and P. D. M. Spelt, "Linear and nonlinear spatio-temporal instability in laminar two-layer flows," J. Fluid Mech. **656**, 458 (2010).
[12] R. Usha and K. C. Sahu, "Interfacial instability in pressure-driven core-annular pipe flow of a Newtonian and a Herschel–Bulkley fluid," J. Non-Newtonian Fluid Mech. **271**, 104144 (2019).
[13] B. Selvam, S. Merk, R. Govindarajan, and E. Meiburg, "Stability of miscible core-annular flows with viscosity stratification," J. Fluid Mech. **592**, 23 (2007).
[14] A. Orazzo, G. Coppola, and L. De Luca, "Disturbance energy growth in core–annular flow," J. Fluid Mech. **747**, 44 (2014).
[15] B. T. Ranganathan and R. Govindarajan, "Stabilisation and destabilisation of channel flow by location of viscosity-stratified fluid layer," Phys. Fluids. Lett. **13(1)**, 1 (2001).
[16] P. Ern, F. Charru, and P. Luchini, "Stability analysis of a shear flow with strongly stratified viscosity," J. Fluid Mech. **496**, 295 (2003).
[17] S. V. Malik and A. P. Hooper, "Linear stability and energy growth of viscosity stratified flows," Phys. Fluids **17**, 024101 (2005).
[18] R. Govindarajan, S. V. L'vov, and I. Procaccia, "Retardation of the onset of turbulence by minor viscosity contrasts," Phys. Rev. Lett. **87**, 174501 (2001).
[19] K. C. Sahu, H. Ding, P. Valluri, and O. K. Matar, "Linear stability analysis and numerical simulation of miscible channel flows," Phys. Fluids **21**, 042104 (2009).
[20] L. Talon and E. Meiburg, "Plane Poiseuille flow of miscible layers with different viscosities: instabilities in the Stokes flow regime," J. Fluid Mech. **686**, 484 (2011).
[21] K. C. Sahu and R. Govindarajan, "Linear stability analysis and direct numerical simulation of two-layer channel flow," J. Fluid Mech. **798**, 889 (2016).
[22] M. Mishra, P. M. J. Trevelyan, C. Almarcha, and A. D. Wit, "Influence of double diffusive effects and miscible viscous fingering," Phys. Rev. Lett. **105**, 204501 (2010).
[23] M. Mishra, A. De Wit, and K. C. Sahu, "Double diffusive effects on pressure-driven miscible displacement flows in a channel," J. Fluid Mech. **712**, 579 (2012).

[24] S. Swernath and S. Pushpavanam, "Viscous fingering in a horizontal flow through a porous medium induced by chemical reactions under isothermal and adiabatic conditions," J. Chem. Phys. **127**, 204701 (2007).
[25] D. Pritchard, "The linear stability of double-diffusive miscible rectilinear displacements in a Hele-Shaw cell," Eur. J. Mech. B, Fluids **28 (4)**, 564 (2009).
[26] K. C. Sahu and R. Govindarajan, "Linear stability of double-diffusive two-fluid channel flow," J. Fluid Mech. **687**, 529 (2011).
[27] K. C. Sahu and R. Govindarajan, "Spatio-temporal linear stability of double-diffusive two-fluid channel flow," Phys. Fluids **24**, 054103 (2012).
[28] S. Ghosh, R. Usha, and K. C. Sahu, "Double-diffusive two-fluid flow in a slippery channel: A linear stability analysis," Phys. Fluids **26**, 127101 (2014).
[29] M. J. South and A. P. Hooper, "Linear growth in two-fluid plane Poiseuille flow," J. Fluid Mech. **381**, 121 (2001).
[30] C. T. Tan and G. M. Homsy, "Stability of miscible displacements: rectangular flow," Phys. Fluid **29**, 73549 (1986).
[31] P. J. Schmid and D. S. Henningson, *Stability and transition in shear flows* (Springer-Verlag New York, Inc, New York, 2001).
[32] C. Canuto, M. Y. Hussaini, A. Quarteroni, and T. Zang, *Spectral Methods in Fluid Dynamics*, 1st ed. (Springer-Verlag, Amsterdam, 1987), pp. 65–70.
[33] R. Govindarajan, "Effect of miscibility on the linear instability of two-fluid channel flow," Int. J. Multiphase Flow **30**, 1177 (2004).
[34] B. Selvam, L. Talon, L. Lesshafft, and E. Meiburg, "Convective/absolute instability in miscible core-annular flow. Part 2. Numerical simulations and nonlinear global modes," J. Fluid Mech. **618**, 323 (2009).
[35] P. G. Drazin and W. H. Reid, *Hydrodynamic stability* (Cambridge University Press, Cambridge, 1985).